UvA-DARE (Digital Academic Repository)

Brain mechanisms of unconscious cognitive control

van Gaal, S.

Publication date
2009

Citation for published version (APA):
van Gaal, S. (2009). *Brain mechanisms of unconscious cognitive control*. [Thesis, fully internal, Universiteit van Amsterdam].

8. Unconscious errors enhance prefrontal-occipital oscillatory synchrony

Abstract

The medial prefrontal cortex (MFC) is critical for our ability to learn from previous mistakes. Here we provide evidence that neurophysiological oscillatory long-range synchrony is a mechanism of post-error adaptation that occurs even without conscious awareness of the error. During a visually signaled Go/No-Go task in which half of the No-Go cues were masked and thus not consciously perceived, response errors enhanced tonic (i.e., over 1-2 seconds) oscillatory synchrony between MFC and occipital cortex leading up to and during the subsequent trial. Spectral Granger causality analyses demonstrated that MFC → occipital cortex directional synchrony was enhanced during trials following both conscious and unconscious errors, whereas transient stimulus-induced occipital → MFC directional synchrony was independent of errors in the previous trial. Further, the strength of pre-trial MFC-occipital synchrony predicted individual differences in task performance. Together, these findings suggest that synchronous neurophysiological oscillations are a plausible mechanism of MFC-driven cognitive control that is independent of conscious awareness.

Introduction

Throughout life, we try to improve our performance on goal-directed tasks, in part by learning from our previous mistakes. Monitoring our actions for errors and fine-tuning performance accordingly is a key function of the cognitive control system, a neural network in which the medial prefrontal cortex (MFC) plays a prominent and crucial role (Carter & van Veen, 2007; Ridderinkhof et al., 2004). Myriad studies spanning several species have implicated the MFC in action monitoring, conflict detection, error signaling, and reinforcement learning (Carter & van Veen, 2007; Nieuwenhuis, Holroyd, Mol, & Coles, 2004). Generally, these studies show that MFC activity increases following errors or negative feedback, and is correlated with adjustments in performance or decision-making in the subsequent trial (Cohen & Ranganath, 2007; Debener et al., 2005; Gehring, Goss, Coles, Meyer, & Donchin, 1993; Ridderinkhof, Nieuwenhuis, & Bashore, 2003).

And yet, little is known about the neurobiological mechanisms by which processes in the MFC can lead to adjustments in performance. Researchers using fMRI have revealed that activity in regions involved in task-relevant stimulus processing is enhanced following errors or conflicts (Egner & Hirsch, 2005). We hypothesize that this top-down control is realized through synchronized

electrophysiological oscillations. Oscillations reflect rhythmic fluctuations in population-level dendritic activity and action potentials, and accompany memory, decision-making, and other cognitive processes (Buzsaki & Draguhn, 2004; Cohen, Elger, & Ranganath, 2007; Engel, Fries, & Singer, 2001; Klimesch, 1999). Further, synchronized oscillations across brain regions have been linked to conditioning and choice behavior (Pesaran, Nelson, & Andersen, 2008; Popescu, Popa, & Pare, 2009; Sauseng & Klimesch, 2008). Here we examined whether long-range neurophysiological oscillatory synchrony is a plausible mechanism by which the MFC engages top-down control over sensory processing following errors.

The adaptive change in cognitive control that occurs after errors has traditionally been conceptualized as an effortful process, requiring conscious awareness that an error was made or negative performance feedback was given. However, conscious awareness may not be necessary for all aspects of cognitive control. Indeed, non-consciously perceived conflict or error signals modulate activity in the motor system (Dehaene et al., 1998) and prefrontal cortex (Hester et al., 2005; Klein et al., 2007; Nieuwenhuis et al., 2001; Ursu et al., 2009). Moreover, some aspects of high-level cognitive control, such as response inhibition and task-switching, may also occur in absence of conscious awareness (Lau & Passingham, 2007; van Gaal et al., 2008). However, such unconscious processes are thought to be ephemeral, lasting only a few hundred milliseconds (Dehaene & Naccache, 2001; Greenwald et al., 1996; Rossetti, 1998). The extent to which unconsciously made errors can engage top-down control remains unknown.

We recorded EEG from human subjects while they performed a visually signaled Go/No-Go task, in which one half of the No-Go cues were presented in a way that evaded conscious awareness. We examined oscillatory phase synchrony—a measure of frequency-band specific functional connectivity—between the MFC and occipital cortex (OCC) on correctly responded Go trials that followed conscious errors, unconscious errors, or other correct Go trials. Enhanced MFC-OCC synchrony occurred on trials following unconscious and conscious errors, and predicted subjects' behavioral performance. Pre-trial synchrony was dominated by an MFC → OCC directional flow; OCC → MFC directed synchrony was maximal following stimulus onset and was unrelated to errors in the previous trial. These findings suggest that the MFC uses synchronized oscillations to entrain sensory regions following errors to improve sensory processing. Further, these findings demonstrate that top-down control over sensory cortex occurs even when errors are made unconsciously.

Materials and Methods

Participants

Subjects were 15 right-handed undergraduate psychology students (14 female) at the University of Amsterdam, with normal or corrected-to-normal vision. Subjects gave written informed consent prior to participation, and the experiment was approved by the local ethical committee.

Task overview

Participants performed a masked Go/No-Go task, in which No-Go signals were presented consciously or unconsciously. They were instructed to press the response button as quickly as possible to the appearance of a black annulus (the Go-signal, duration 100 ms, 2.17 cd/m², visual angle of 1.30°). On 15% of trials, a No-Go signal (grey circle, duration 16.7 ms followed by a 67 ms delay, 41.85 cd/m², visual angle of 0.60°) preceded the Go-signal, indicating that subjects must withhold their response. On another 15% of trials, an undetectable No-Go cue (the same grey circle, duration 16.7 ms with no delay) was presented (see Figure 8.1a). This cue was undetected because the subsequent Go signal functioned as a metacontrast mask that successfully prevented the No-Go cue from reaching conscious awareness (van Gaal et al., 2008). Trial duration was jittered between 1400 and 2200 ms (in steps of 200 ms), randomly drawn from a uniform distribution, rendering the presentation of the stimuli temporally unpredictable.

The experiment consisted of three sessions on separate days; two behavioral testing sessions (1, 2) and an EEG recording session (3). Participants performed seven experimental blocks per session, each containing 200 trials (140 Go trials, 30 conscious No-Go trials and 30 unconscious No-Go trials). After each block, participants received performance feedback (mean RT, percentage correct stops on conscious No-Go trials). They were not informed about the presence of unconscious No-Go trials. Stimuli were presented on a grey box (59.1 cd/m², visual angle of 3.78°) against a black background (2.17 cd/m²) at the center of a 15-inch BenQ TFT monitor with a refresh rate of 60 Hz. The monitor was placed at a distance of approximately 90 cm in front of the participant, so that each centimeter subtended a visual angle of ~0.64 degrees. The experiment was programmed with Presentation (Neurobehavioral Systems, Albany, USA).

Experiment conditions

We distinguished three types of trials: Go trials following correct Go trials ("Go"); Go trials following trials that contained a visible No-Go cue, but in which subjects

committed a response ("conscious errors"); and Go trials following trials that contained a masked No-Go cue, but in which subjects committed a response ("unconscious errors") (see Figure 8.1a). Note that all trials included in the present analyses are Go trials, and that there was a response on the previous trial; differences among conditions lie solely in whether the previous trial contained a conscious, nonconscious, or no No-Go cue. Further, because the unconscious No-Go cue on previous trial did not reach subjective awareness, Go trials following other Go trials are also identical to Go trials following unconscious errors in terms of the subjective experience.

Visibility of No-Go signals

To test whether subjects were truly unaware of the unconscious No-Go signals, they performed two discrimination tasks after the main task. In both tasks, the stimulus display and trial timing were identical to the main task. In the first yes/no detection task, the number of trials per condition was the same as one block in the Go/No-Go task (140 Go trials, 30 unconscious No-Go trials, 30 conscious No-Go trials). However, subjects were instructed to press a button only when they perceived a No-Go signal. In the second, more conservative, forced-choice discrimination task (2 blocks of 100 trials), subjects were informed about the presence of a very brief No-Go signal shortly before the Go signal on some trials. No participants reported awareness of these No-Go signals during the Go/No-Go experiment. In this task, each block consisted of 50 unconscious No-Go trials and 50 Go trials (pseudo-random order). Participants were instructed to press the left button when they thought a brief No-Go signal preceded the Go signal and to press the right button when they thought this was not the case. Participants were told that in 50% of all trials, a Go signal was preceded by a No-Go signal and were instructed to consider this in their response.

EEG recording and processing

EEG data were recorded at 256 Hz using a BioSemi ActiveTwo amplifier from 48 scalp electrodes and 4 peri-occular electrodes. All analyses were conducted in Matlab, using in-house written code supplemented by EEGLAB (Delorme & Makeig, 2004) (independent components analysis and topographical plotting) and BSMART (Cui, Xu, Bressler, Ding, & Liang, 2008) (spectral Granger causality estimates). Data were re-referenced off-line to the average of the activity recorded at the two ear lobes. All data were visually inspected, and trials containing artifacts were identified and removed. Blink artifacts were removed from the data using independent

components analyses in EEGLAB. EEG data were first current-source-density transformed (Kayser & Tenke, 2006) to increase spatial selectivity and minimize volume conduction (contribution of deep sources that project to many electrodes). For analyses with pooled data, unfiltered time-domain EEG data were averaged together from FC1, FCz, and FC2, and from O1, Oz, and O2. For convenience, we refer to these pooled electrodes as MFC and OCC, respectively. Pooling data across several electrodes has the advantage of increasing signal-to-noise ratio and minimizing any possible noise fluctuations in a single electrode. We also conducted all analyses using a single electrode (FCz and Oz); the pattern of results was the same as those reported here.

Phase synchrony analyses

Phase synchrony was computed first by extracting the phase angle time series from the data via complex Morlet wavelet convolution (Cavanagh, Cohen, & Allen, 2009; Cohen et al., 2009), and computing the magnitude of the average phase angle difference between two electrodes over trials at each time/frequency point. Data were first convolved with a family of complex Morlet wavelets, defined as $e^{i2\pi f}e^{-t^2/(2*\sigma^2)}$, where t is time, f is frequency, which increased from 2 to 60 Hz in 50 logarithmically spaced steps. σ defines the width of each frequency band, and was set according to 4/(2πf). Power is defined as the modulus of the resulting complex signal Z_t (real$[z_t]^2$ + imag$[z_t]^2$), and phase angle is defined as arctan(imag$[z_t]$/real$[z_t]$). Inter-site phase synchrony (Lachaux, Rodriguez, Martinerie, & Varela, 1999) measures the extent to which oscillation phase angle differences between electrode pairs are consistent over trials at each time/frequency point, and vary from 0 (completely random phase angle differences across trials) to 1 (identical phase angle differences across trials): $|\frac{1}{n}*\sum_{t=1}^{n}e^{i[\phi_{jt}-\phi_{kt}]}|$, where n is the number of points, and ϕ_j and ϕ_k are the phase angles of electrodes j and k.

Statistics were conducted in two ways. First, we computed paired-sample t-tests on the differences between conditions in the 2-12 Hz band at each time point across subjects (Figure 8.2b). This frequency band was selected based on the condition-averaged synchrony plot (Figure 8.2a), and on the spectral Granger causality plots (Figure 8.4a). Temporal regions were highlighted if each time point achieved a significance of $p < 0.05$, with at least 40 contiguous significant samples (156 ms). These analyses are mainly for illustration purposes. Results were confirmed through repeated-measures ANOVAs, in which average synchrony was

taken from 3 temporal windows (first averaging from 2-12 Hz): -1200 to -300 ms preceding stimulus onset, 100 to 300 post-stimulus onset (MFC-OCC synchrony peaked at 200 ms; we refer to this time window as "peak synchrony"), and 500 to 1400 ms post-stimulus onset. These windows were selected to examine activity pre-trial, peak synchrony, and post-trial. Repeating the analyses using different time windows did not appreciably alter the results. Averaged data were entered into a 3 (condition) X 3 (time window) repeated-measures ANOVA. Greenhouse-Geisser correction for nonsphericity was used; for ease of interpretation, uncorrected degrees of freedom are reported.

Topographical (whole-head) synchrony analyses

In these analyses, phase synchrony was computed over trials between each possible electrode pair within a frequency band of 2-12 Hz, as described above. Here, we extracted phase angles by applying the Hilbert transform to band-pass filtered data (Le Van Quyen et al., 2001). To pool these data, we averaged the phase synchrony values for each condition among FC1, FCz, and FC2, and among O1, Oz, and O2. Statistics were performed by computing a paired-sample t-test across subjects at each electrode for differences between conditions. Any electrode that was not significant at $p < 2.22 \times 10^{-5}$ (corresponding to 0.001 with Bonferroni correction for 45 electrodes) was assigned a value of 0 (grey in Figure 8.3a-b).

Spectral Granger causality

Spectral Granger causality estimates the amount of variance in signal X that can be explained by activity in signal Y previously in time, at a particular frequency band. It was implemented here using Matlab code available in the BSMART toolbox (Cui et al., 2008), which has previously been validated for neurophysiological data (Gaillard et al., 2009; Zhang, Chen, Bressler, & Ding, 2008). Time-domain, unfiltered data from prefrontal and occipital sites were pooled prior to the analyses, as described above. Statistics were performed using a repeated-measures ANOVA, as described for the phase synchrony analyses.

Brain-brain and brain-behavior correlations

For correlations between pre-trial and synchrony peak activity, we used robust regression (Holland & Welsch, 1977) as implemented in the statistics toolbox in Matlab. Robust regression uses an iterative weighting least-squares approach to minimize the contribution of potential outliers, and minimizes the possibility of finding statistically significant relationships that are driven by a small number of

data points. For correlations between synchrony and task performance, we computed an "efficiency" index (Townsend & Ashbey, 1983) by dividing the average response time on Go trials by one minus the proportion of errors on conscious No-Go trials (i.e., the inhibition rate). Response times from error trials were not included because they are faster than correct responses and thus may introduce bias. This provides a composite performance measure that takes into account both correct responses and successful inhibition rates. Correlations were computed using Spearman's rho.

Results

Visibility of No-Go signals

To probe visibility of the No-Go cues, subjects performed two discrimination tasks following the main experiment (see Methods for details). In the first yes-no detection task, which had the same stimulus presentation parameters as the main task, the hit rate of 2% on unconscious No-Go trials did not exceed the false alarm rate of 0.8% on Go trials (the hit rate on conscious No-Go trials was 93.3%). In the second, more conservative forced-choice discrimination task, subjects were explicitly informed about the presence of a brief No-Go signal during some trials, and that these would occur on 50% of trials. Also in this task, participants were unable to discriminate between Go trials and unconscious No-Go trials (d' = 0.05, mean percentage correct = 51%), as evidenced by chance-level performance ($p > 0.2$ for both discrimination tasks, see (van Gaal et al., 2008) for more details).

Unconscious No-Go cues slow response times on subsequent trials

Although the unconscious No-Go cue was not perceived, subjects were slower on Go trials following unconscious errors, compared to Go trials following Go trials (Figure 8.1b). Although small in magnitude (on average 3.1 ms), this effect was reliable across participants and testing sessions ($F(1,14)$ = 5.98; p = 0.028). Subjects also were slower on Go trials following conscious errors (on average 19.6 ms; $F(1,14)$ = 13.45; p = 0.003), which replicates many previous post-error slowing studies.

MFC-OCC synchrony following response errors

We examined oscillatory phase synchrony between a pool of prefrontal electrodes (FC1, FCz, and FC2; hereafter referred to as MFC) and a pool of occipital electrodes (O1, Oz, O2; hereafter referred to as OCC); pooling ensures high signal-to-noise and minimal chance of finding effects due to noise fluctuations in any single electrode. Data were first current-source-density transformed to maximize spatial resolution

and minimize volume conduction. When averaging across conditions, we found a strong 'burst' of MFC-OCC synchrony around 100-400 ms following the onset of the Go stimulus, in a relatively broad low-frequency range of about 2-12 Hz (Figure 8.2a). Based on the experimental design and time-course of inter-site phase synchrony, we defined three time windows of interest for subsequent investigations: "pre-trial" (-1200 to -300 ms before stimulus onset), "peak synchrony" (100 to 300 ms following stimulus onset; peak synchrony was observed at ~200 ms), and "post-trial" (500 to 1400 ms following stimulus onset).

A) Task design

B) Post-error slowing
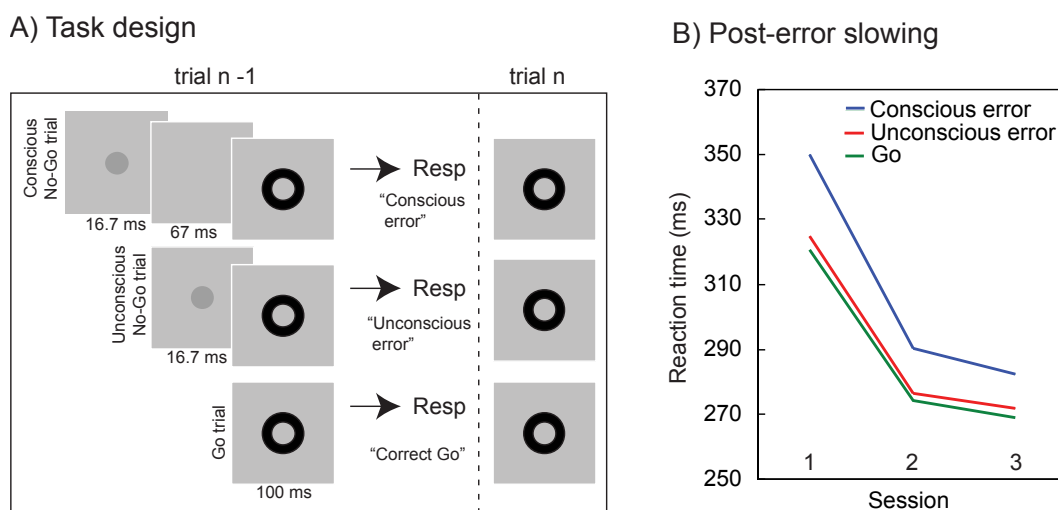
Figure 8.1 Overview of task design and behavioral results

(a) Visual representation of trial events for the three conditions. Note that all data reported here are from correctly responded Go trials ("trial n") in which the previous trial also contained a response, separated according to whether the previous trial contained a consciously visible No-Go cue ("conscious error", top), an unconsciously presented No-Go cue ("unconscious error", middle), or a Go cue ("correct go", bottom). (b) Subjects were significantly slower on Go trials following unconscious and conscious errors than on Go trials following correct Go trials, over two behavioral testing sessions (1, 2), and the EEG recording session (3).

Upon closer inspection of patterns of MFC-OCC synchrony in different conditions, we found that when subjects committed either conscious or unconscious errors in the previous trial, MFC-OCC synchrony significantly increased, both before the trial started and throughout the trial (with the exception of the time of the peak synchrony, around 200 ms post-stimulus; see Figure 8.2b). A 3 (condition) X 3 (time window: pre-trial, peak synchrony, post-trial) repeated-measures ANOVA confirmed the significant main effects of condition ($F(2,28) = 78.5$, $p < 0.001$) and time window ($F(2,28) = 46.78$, $p < 0.001$), and a significant condition*time window interaction ($F(4,56) = 4.33$, $p = 0.021$), which was driven by differences among conditions being smaller immediately following stimulus onset (100 to 300 ms). During the pre-

stimulus period, MFC-OCC synchrony was significantly stronger for trials following unconscious errors compared to trials following Go trials ($t(14) = 8.1$, $p < 0.001$), and for trials following conscious errors compared to trials following Go trials ($t(14) = 8.5$, $p < 0.001$). Trials following conscious errors also had significantly stronger synchrony compared to trials following unconscious errors ($t(14) = 6.1$, $p < 0.001$). The pattern of results was not affected by our choice of frequency band, because similar effects were observed when using narrower frequency ranges (see Supplemental Figure S1). These results could also not be due to an alternative explanation of differences in oscillation power (which may affect estimates of phase synchrony), because oscillation power effects at either MFC or OCC did not mirror synchrony effects, nor were synchrony and power significantly correlated across subjects (see Supplemental Figure S2).
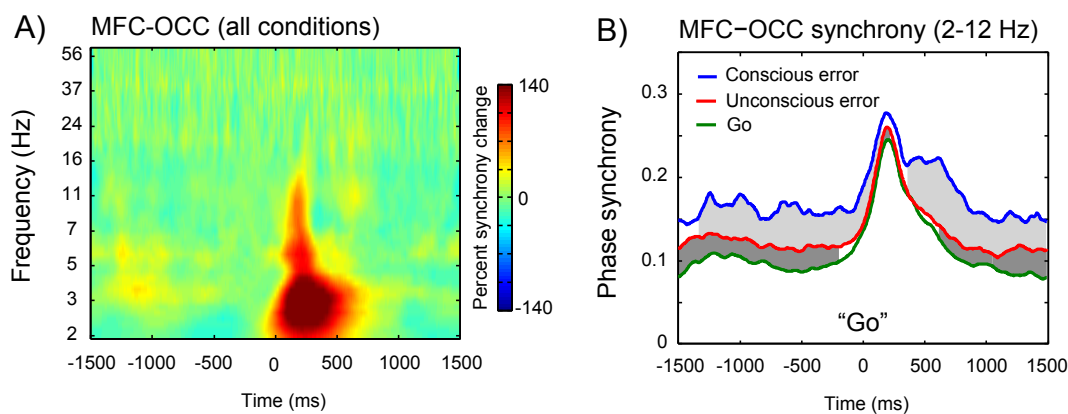
Figure 8.2 Oscillatory phase synchrony between prefrontal and occipital electrode sites

Oscillatory phase synchrony between prefrontal and occipital cortices was significantly enhanced following unconscious and conscious errors. (a) Time-frequency plot of oscillatory phase synchrony averaged across all conditions demonstrates a 'burst' of synchrony between a pool of medial frontal electrodes (MFC) and a pool of occipital electrodes (OCC) from around 2-12 Hz following the onset of the Go stimulus (data are converted to percent change from a -300 to -100 ms baseline at each frequency). (b) Oscillatory phase synchrony from 2-12 Hz plotted separately for each condition (values are the magnitude of the average projection vector over phase angle differences; see Methods). Phase synchrony was significantly stronger following unconscious and conscious errors compared to Go trials, and was significantly stronger following conscious compared to unconscious errors. Grey regions reflect time windows in which at least 156 contiguous ms (40 samples) survived a paired-samples t-test at p < 0.05 (see text for complementary results from ANOVAs).

This set of analyses demonstrated that oscillatory synchrony between MFC and OCC increases following conscious and unconscious errors, extending several seconds after the error into the following trial. These analyses were anatomically constrained according to our a priori hypotheses regarding the roles of medial prefrontal and occipital cortices in the visually cued Go/No-Go task; in the next set of analyses, we

examine the topographical distribution of post-error oscillatory functional connectivity.

Topographical analyses of phase synchrony.

To examine the more global spatial distribution of these effects, we computed inter-site synchrony between MFC and all other electrodes, and between OCC and all other electrodes, for each condition and for the three time windows of interest (pre-trial, peak synchrony, and post-trial). To remove global patterns of inter-regional synchrony, we subtracted seeded synchrony maps during Go trials following Go trials, from Go trials following unconscious and conscious errors. As seen in Figure 8.3a-b, synchrony between the OCC seed and prefrontal regions was significantly greater during trials following both unconscious and conscious errors compared to trials following Go trials; similarly, synchrony between the MFC seed and occipital regions was significantly greater following errors compared to following Go trials. To threshold these maps statistically, a paired-samples t-test was conducted at each electrode across subjects; electrodes with synchrony differences that were not significant at $p < 2.22 \times 10^{-5}$ (0.001 with Bonferroni correction for 45 electrode pairs) had their values set to zero (grey color). MFC-OCC synchrony differences were prominent pre-trial and post-trial; in contrast, strong topographical differences were not observed during the time of stimulus-related activity (100-300 ms).
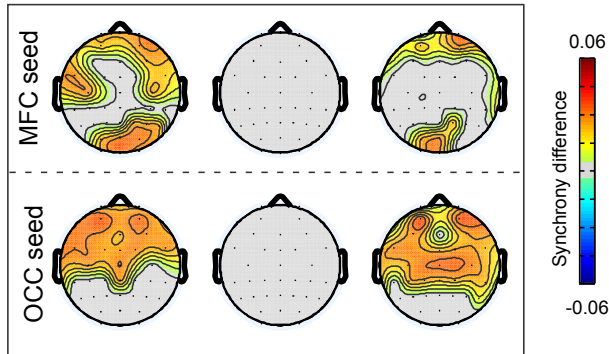
These findings confirm the specificity of long-range, prefrontal-occipital synchrony following unconscious and conscious errors. As seen in Figure 8.3c, current-source-density transform was successful at minimizing the effects of volume conduction; when averaging across conditions, phase synchrony was strong only with the electrodes used for pooling, and was minimal even with neighboring electrodes.

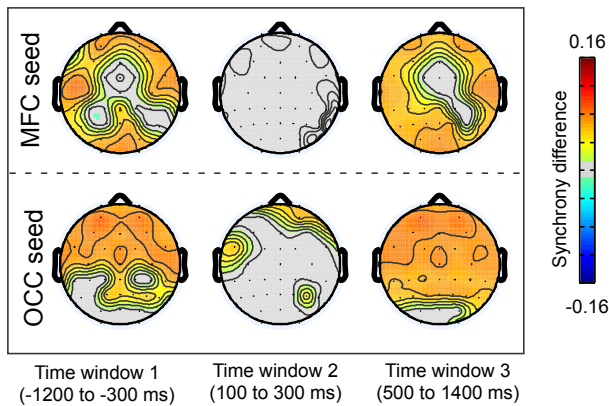*Directional influences estimated from spectral Granger causality*

In our next set of analyses, we used spectral Granger causality to estimate the directional influence of the MFC-OCC interactions. Go trials following errors had significantly enhanced pre-trial MFC → OCC directional synchrony compared to trials following Go trials (Figure 8.4a). A 3 (condition) X 3 (time window) repeated-measures ANOVA revealed a significant main effect of condition ($F(2,28) = 9.58$, $p = 0.003$), and no effect of or interaction with time window (p's > 0.4). Follow-up t-tests confirmed that during the pre-trial time window, unconscious ($t(14) = 2.64$, $p = 0.019$) and conscious ($t(14) = 3.6$, $p = 0.003$) errors elicited greater MFC → OCC directional synchrony compared to Go trials. In contrast, OCC → MFC directional

synchrony was not statistically significantly modulated by events in the previous trial ($F(2,28)$ = 2.62, p = 0.12). There was a main effect of time, with OCC → MFC directional synchrony being maximal in the 100-300 ms time window ($F(2,28)$ = 5.27, p = 0.03; see Figure 8.4b).

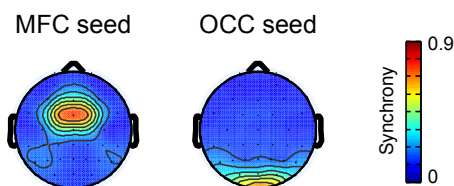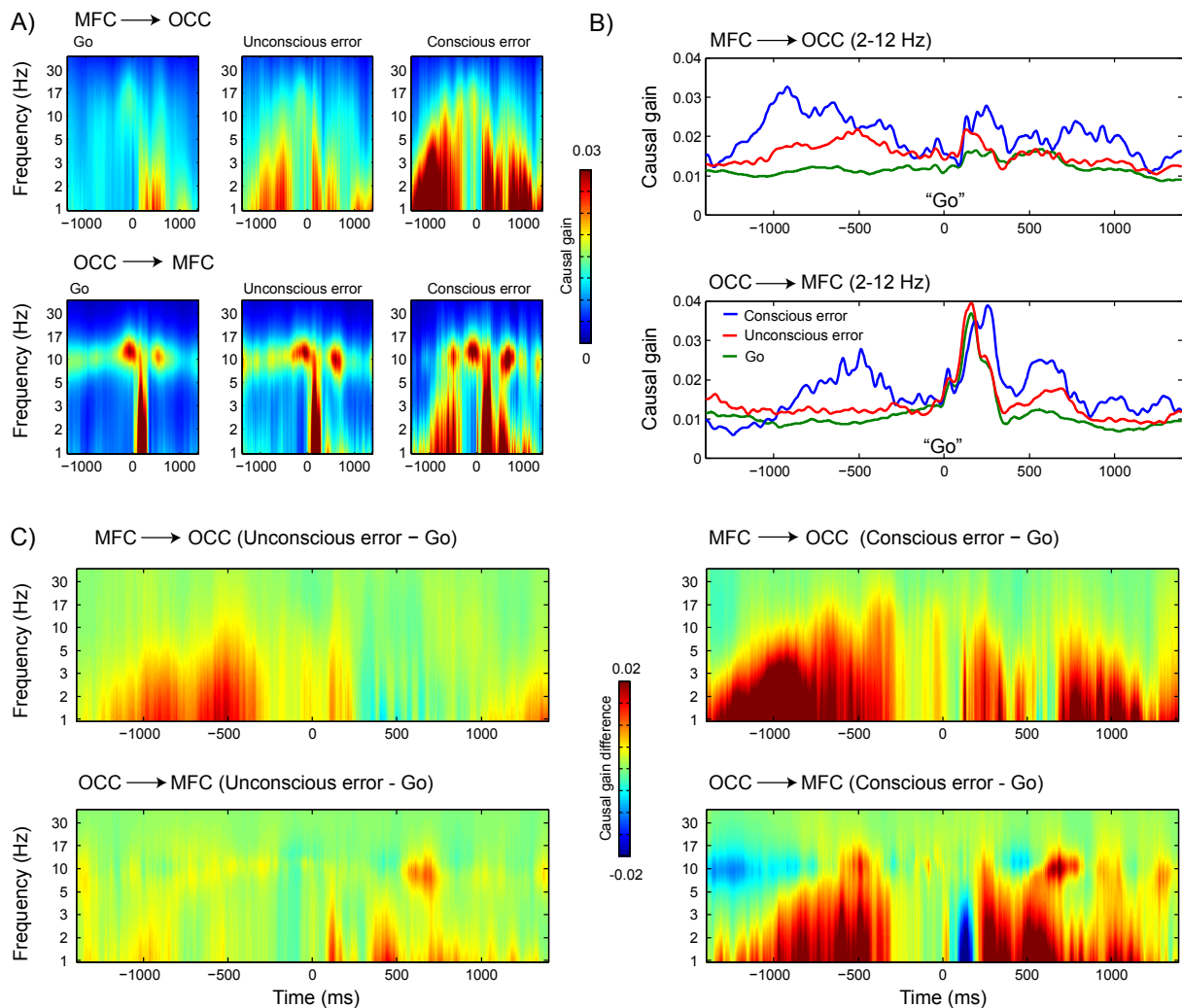**A) Unconscious error - Go**

B) Conscious error - Go

Time window 1 (-1200 to -300 ms)   Time window 2 (100 to 300 ms)   Time window 3 (500 to 1400 ms)

C) All conditions

MFC seed   OCC seed

Figure 8.3 Topographical analyses of oscillatory phase synchrony

*Topographical analyses of oscillatory phase synchrony reveal spatial distribution of frontal-occipital connectivity following unconscious and conscious errors. In these analyses, phase synchrony between the MFC seed and every other electrode (top row of **A** and **B**), and between the OCC seed and every other electrode (bottom row of **A** and **B**) was calculated; differences between trials following unconscious errors and Go trials (a) and between trials following conscious errors and Go trials (b) are plotted. Electrodes with differences not statistically significant at p < 2.22*10^-5 had their values set to 0 (grey color). It can be seen that the MFC seed was significantly more strongly synchronized with occipital regions, and that the OCC seed was significantly more strongly synchronized with frontal regions, following unconscious and conscious*

errors. (c) Synchrony with MFC and OCC seeds when averaging across all time windows and conditions. These plots show that there is minimal contribution of volume conduction due to current-source-density transform.

Figure 8.4 Directional influences estimated from spectral Granger causality

Spectral Granger causality reveals both top-down (MFC→OCC) directed influence, which was significantly increased following unconscious and conscious errors, and bottom-up (OCC→MFC) influence, which was strongest during stimulus presentation and was not modulated by the previous trial. (a) Time-frequency plots for each condition for MFC→OCC directed synchrony (top row) and OCC→MFC directed synchrony (bottom row). Deeper red colors indicate that more variance in OCC (top) or MFC (bottom) can be explained by variance in MFC (top) or OCC (bottom) in each band. Pre-stimulus MFC→OCC directed synchrony was significantly enhanced following unconscious and conscious errors. In contrast, OCC→MFC was strongest during stimulus presentation, but was not significantly modulated by events in the previous trial. (b) Line plots (average from 2-12 Hz) demonstrates time course of directed synchrony effects. (c) Difference maps between trials following unconscious errors and Go trials (left side) and between trials following conscious errors and Go trials (right side) demonstrates time-frequency regions in which condition differences were maximal.

Further ANOVAs confirmed that during the pre-trial period, there was a significant directionality X condition interaction ($F(2,28) = 7.17$, $p = 0.01$), such that MFC → OCC synchrony was characterized by a significant increase in synchrony strength from trials following correct Go trials, to those following unconscious errors, to those following conscious errors ($F(1,14) = 6.97$, $p = 0.019$) (Figure 8.4c). In contrast, pre-trial OCC → MFC directional synchrony was not significantly different among the three conditions ($F(1,14) = 2.79$, $p = 0.11$).

These spectral Granger causality analyses revealed both "bottom-up" (OCC → MFC) and "top-down" (MFC → OCC) directional coupling; pre-trial synchrony was dominated by an MFC → OCC flow and was significantly enhanced by conscious and unconscious errors on the previous trial. In contrast, OCC → MFC flow was strongest shortly after stimulus onset, and was not significantly modulated by errors in the previous trial. These findings are consistent with the idea that the prefrontal cortex uses oscillatory synchrony to "instruct" visual cortex to improve sensory processing. We therefore hypothesized that pre-trial top-down directed synchrony should predict the strength of subsequent bottom-up directed synchrony.

To test this, we regressed pre-trial MFC → OCC directed synchrony (from the spectral Granger causality analyses) on peak synchrony OCC → MFC directed synchrony. We found significant positive relations in all conditions, indicating that individuals with stronger pre-trial MFC → OCC directed synchrony had stronger OCC → MFC directed synchrony during subsequent stimulus presentation (Figure 8.5a). This was confirmed using robust regression ($t(13)$: 2.91, 2.1, and 2.22; p-values: 0.01, 0.05, and 0.04 for trials following Go, conscious errors, and unconscious errors). These effects were not due to an alternative explanation of general stable levels of synchrony across subjects, because the strength of pre-trial OCC → MFC synchrony did not predict the strength of peak synchrony MFC → OCC synchrony (all p's > 0.17) (Figure 8.5a).

Top-down synchrony strength predicts inhibition performance
In our final set of analyses, we examined the link between MFC-OCC oscillatory phase synchrony and behavioral performance. We computed a unitary performance measure that takes into account both speed (response times on correctly responded Go trials) and accuracy (errors on No-Go trials). For each subject, we divided the average response time to Go trials by the conscious No-Go inhibition rate (see Methods); thus, subjects with lower numbers are better performers. We then correlated this efficiency measure with oscillatory phase synchrony, and found that subjects with stronger MFC-OCC phase synchrony during Go trials following

conscious errors performed significantly better on the task (Figure 8.5b) (Spearman's rho: -0.56, -0.63, and -0.74, p-values: 0.03, 0.01, and 0.002, for pre-trial, peak synchrony, and post-trial). These correlations remained significant when excluding the possible outlier from the correlations (p-values: 0.02, 0.01, and 0.01). As seen in Figure 8.5b inset, synchrony-performance correlations became increasingly negative from Go trials following Go, to those following unconscious errors, to those following conscious errors. We also computed correlations between MFC-OCC synchrony and post-error reaction time slowing, but no correlations were significant (all p's > 0.2). No correlations between MFC-OCC synchrony and average reaction time on Go trials (not scaled by inhibition rate) were significant (all p's > 0.23). In other words, the strength of MFC-OCC phase synchrony predicted task performance, but was not correlated with overall motor speed.
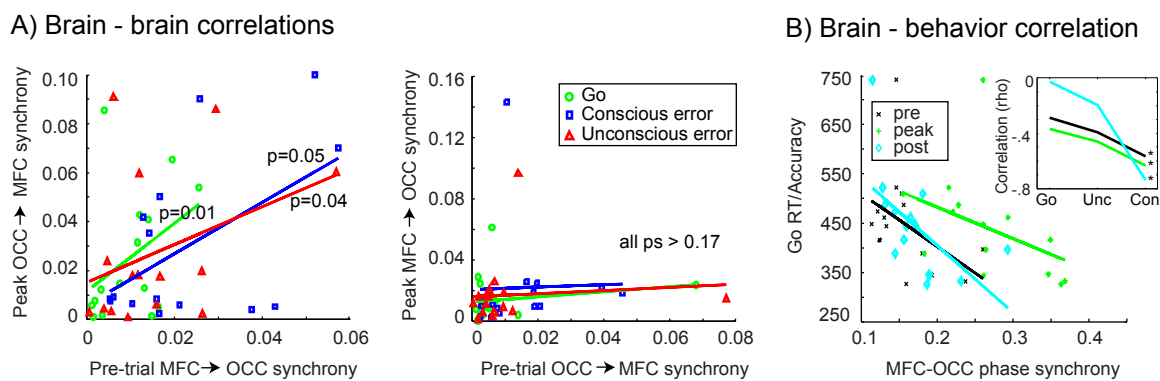
Figure 8.5 Brain-brain and brain-behavior correlations

Correlations between pre-stimulus (-1200 to -300 ms) MFC-OCC synchrony and peak synchrony (100 to 300 ms) OCC activity provide evidence of a prefrontal-mediated top-down control process. (a) Subjects with stronger pre-stimulus MFC→OCC directed synchrony also had stronger peak synchrony OCC→MFC directed synchrony. This was statistically significant in all conditions. (b) In contrast, pre-stimulus OCC→MFC directed synchrony was not significantly correlated with MFC→OCC directed synchrony, demonstrating the specificity of pre-trial top-down control. (c) Subjects with stronger MFC-OCC phase synchrony performed significantly better on the task (using a unitary performance measure that takes into account both response times on Go trials, and inhibition rate; smaller numbers indicate better performance). These synchrony-performance correlations were significant following conscious error trials, and increased in magnitude from Go trials following Go trials, to Go trials following unconscious errors, to Go trials following conscious errors (see inset; asterisks indicate statistical significance at p < 0.05).

Discussion

Learning to adapt behavior following mistakes is critical to our biological and social survival in a fast-paced, ever-changing world. Although considerable evidence points to a role of the MFC in detecting errors or negative feedback and adapting

subsequent performance (Carter & van Veen, 2007; Cohen, 2008; Ridderinkhof et al., 2004; Yeung, Botvinick, & Cohen, 2004), less is known about the mechanisms by which the prefrontal cortex is able to adapt performance. Our results suggest that one mechanism by which MFC adapts performance following errors is by engaging top-down control mechanisms to increase the tuning or efficiency of stimulus processing. This top-down control might be expressed through synchronized electrophysiological oscillations. This is consistent with, and offers a neurobiologically plausible mechanism for, previous neuroimaging work suggesting that prefrontal cognitive control mechanisms amplify cortical responses to task relevant information in sensory cortex (Crottaz-Herbette & Menon, 2006; Egner & Hirsch, 2005; Scerif, Worden, Davidson, Seiger, & Casey, 2006).

Long-range synchronized oscillations are thought to reflect a mechanism by which spatially disparate neural networks become functionally connected, and neural activities across regions are coordinated (Engel et al., 2001; Fries, Nikolic, & Singer, 2007; Kasanetz, Riquelme, O'Donnell, & Murer, 2006). Oscillatory synchrony between widespread brain regions has been linked to learning (Popescu et al., 2009), decision-making (Gaillard et al., 2009; Pesaran et al., 2008), visual priming (Ghuman, Bar, Dobbins, & Schnyeri, 2008), and memory retrieval (Summerfield & Mangels, 2005). The present findings provide novel evidence that such long-range communication may underlie a cognitive control process by which top-down regulation over sensory regions is triggered by response errors.

Spectral Granger causality revealed separable top-down and bottom-up directional synchrony. Bottom-up (OCC → MFC) directional coupling was strongest immediately following the onset of the visual stimulus, whereas top-down (MFC → OCC) directional coupling was strong before the trial began, and again from 500 to 1400 ms following stimulus onset. Interestingly, top-down directional coupling was observed in a relatively lower frequency range whereas bottom-up directional coupling was additionally observed in higher frequencies (alpha, around 8-13 Hz). This finding is consistent with electrophysiological recordings in monkeys (Buschman & Miller, 2007), which show that bottom-up (in that report, parietal → prefrontal) synchronization occurs in a higher frequency band compared to top-down synchronization. Together, these findings suggest that different kinds of information in the brain may be transferred using different frequency bands.

Interestingly, this top-down control mechanism is activated even in absence of conscious awareness that an erroneous response was made to an unconscious No-Go cue. Previous studies have demonstrated that unconscious errors or conflict can increase activity in the MFC (Hester et al., 2005; Klein et al., 2007; Nieuwenhuis et al.,

2001; Ursu et al., 2009). However, the implications of such unconsciously triggered activity increases have thus far remained unknown. Some researchers have suggested that such unconscious errors do not induce post-error or post-conflict performance adjustments (Klein et al., 2007; Kunde, 2003; Nieuwenhuis et al., 2001), although it is possible that the magnitude of the effect is relatively subtle. Importantly, our EEG synchrony results demonstrate that unconscious errors are able to activate the same top-down control mechanism that is activated by conscious errors. This provides an important new window into the extent to which unconscious processes can affect high-level cognitive control processes.

It may seem surprising that MFC-OCC synchrony was sustained over an unusually long time-window (1-2 seconds); results from masked priming studies suggest that the effects of unconscious stimuli on behavior and brain activity are ephemeral, and typically decay within ~500 ms (Dehaene & Naccache, 2001; Greenwald et al., 1996; Rossetti, 1998). Our results demonstrate that not only do unconscious errors enhance activity over MFC, they also activate top-down tonic control processes that extend over several seconds, even following the Go cue in the current trial. The duration of this effect is consistent with recent studies showing that masked (unconscious) words modulate neural activity up to approximately one second after stimulus presentation (Naccache et al., 2005; Gaillard et al., 2009). Even longer effects of unconscious priming (several minutes) have been reported, for example in the "mere exposure" effect (Elliott & Dolan, 1998; Gaillard et al., 2007). The combination of these results suggests that unconscious information can influence cognitive processes for longer periods of time than previously thought. This has implications for an ongoing debate about the neural correlates of conscious and unconscious information processing (Dehaene & Naccache, 2001; Lamme, 2003, 2006).

Although MFC plays a prominent role in adaptive behavior, error processing, and cognitive control (Carter & van Veen, 2007; Ridderinkhof et al., 2004), other prefrontal regions also contribute to executive functioning, including lateral prefrontal cortex. Patterns of synchrony between OCC and a pooled right lateral prefrontal group (electrodes AF4, F4, and FC6) were somewhat similar to OCC synchrony with MFC, but overall less robust (Supplemental Figure S3). Further work will be required to dissociate the contributions of medial versus lateral prefrontal regions during No-Go error adjustments.

Our findings cannot be due to differences in overall oscillation power, because the effects in the power domain did not mirror the MFC-OCC synchrony effects, nor were power changes correlated with inter-site synchrony (see Supplemental

Material). More generally, this dissociation between inter-site synchrony and power demonstrates that important insights into neurocognitive function can be gained from an examination of the interactions among brain regions; in some cases, limiting analyses to average activity in localized brain regions may miss important information. This set of analyses also revealed an important advantage of electrophysiological measures such as EEG and MEG over functional MRI; functional MRI cannot resolve interactions on such short time scales, nor can it be used to determine oscillatory characteristics of brain activity (Axmacher, Elger, & Fell, 2009).

In conclusion, we have provided novel evidence that the prefrontal cortex utilizes oscillatory synchrony as a means of enacting top-down control over sensory regions to enhance stimulus processing. This mechanism is engaged even in absence of conscious awareness that an error was made.

Supplementary material

One potential alternative explanation of changes in phase synchrony is that with increased oscillation power, phase values are better estimated, and this may spuriously increase phase synchrony. However, such an account does not explain our findings: There was no significant main effect of or interaction with condition with occipital oscillation power (p's > 0.5), nor was there a main effect of condition with MFC power ($F(2,28) = 2.57$, $p = 0.115$). There was a time window*condition interaction for MFC power ($F(4,56) = 15.28$, $p < 0.001$), which was driven by increased power following conscious error trials ($t(14) = 4.2$, $p = 0 .001$). This was due to enhanced MFC activity during conscious response errors on the preceding trial (the error-related negativity); indeed, the response on the previous trial occurred on average around 1500 ms before stimulus onset of the current trial.

The alternative explanation of power driving phase synchrony differences also predicts that individual differences in power would be correlated with individual differences in synchrony. However, we found no evidence for such an effect: The difference in inter-site phase synchrony between unconscious errors and Go trials was not significantly correlated with the difference in power between these conditions at MFC (rho = 0.089, $p = 0.75$) or OCC (rho = -0.07, $p = 0.79$); correlations between power and synchrony were also not significantly correlated when comparing trials following conscious errors and Go trials at MFC (rho = -0.09, $p = 0.73$) or OCC (rho = 0.14, $p = 0.60$). Further, inter-site synchrony did not correlate with OCC or MFC power in any condition independently (not computing condition differences) (all p's > 0.35). The lack of complementary effects in power or

significant power-synchrony correlations demonstrate that there is information available in the synchrony across sites beyond what is available at either site alone.
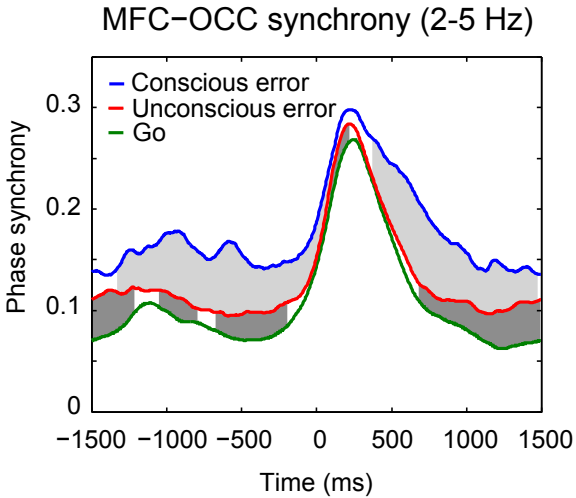
Figure S1. MFC-OCC oscillatory phase synchrony (2-5 Hz)

MFC-OCC oscillatory phase synchrony using a more narrow frequency range (2-5 Hz, compared to 2-12 Hz in Figure 8.2 in the main text). Light grey areas indicate statistical significance at p < 0.05, minimum 156 ms contiguously significant points (40 samples), between Conscious Error and Unconscious error trials. Dark grey area indicates significance between Unconscious Error and Go trials.
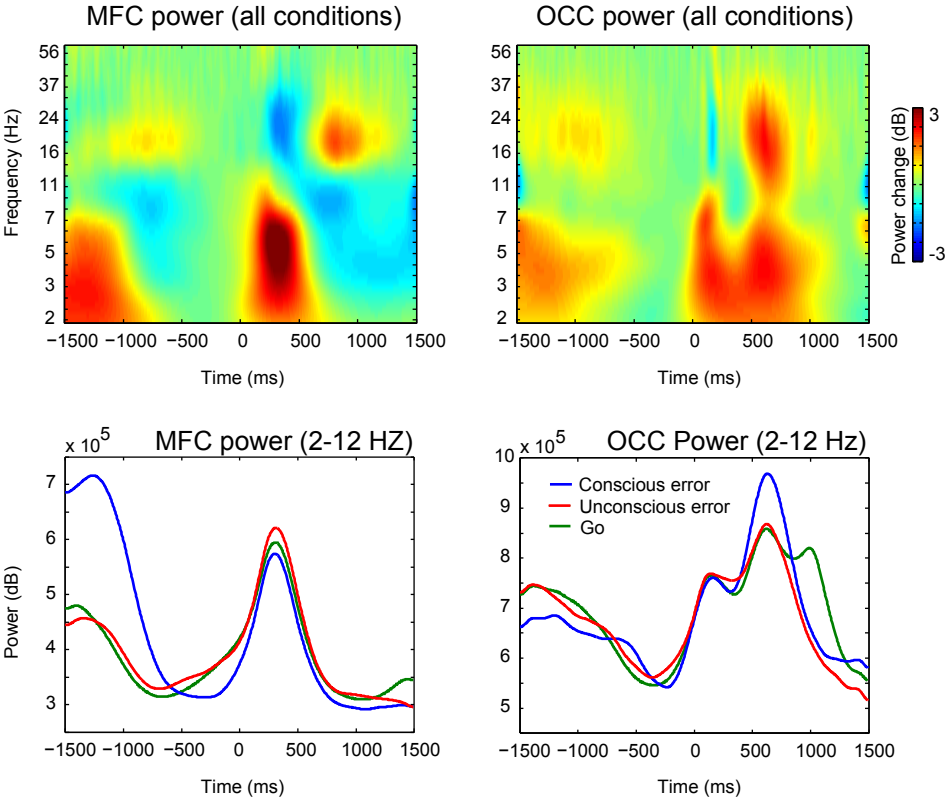
Figure S2. Oscillation power in MFC (left) and OCC (right).
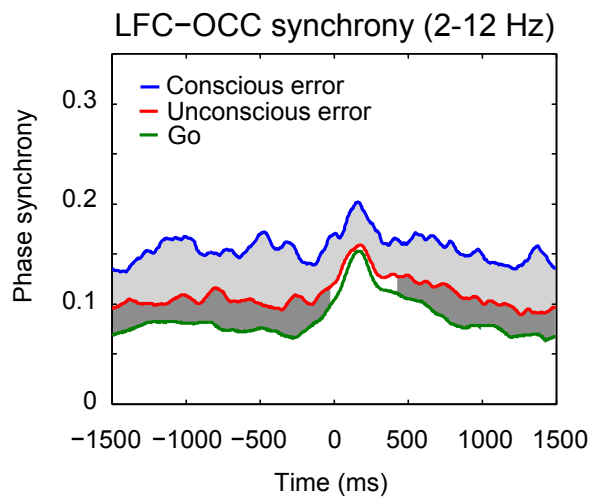
Figure S3. Oscillatory synchrony between OCC and LPFC

Oscillatory synchrony between OCC and a pool of lateral prefrontal sites (AF4, F4, and FC6). Conventions are as in Figure 8.2a in the main text.